Higher-Order Localized Waves in Coupled Nonlinear Schrödinger Equations *

WANG Xin(王鑫)[1], YANG Bo(杨波)[1], CHEN Yong(陈勇)[1**], YANG Yun-Qing(杨云青)[2]

[1]*Shanghai Key Laboratory of Trustworthy Computing, East China Normal University, Shanghai 200062*

[2]*School of Mathematics, Physics and Information Science, Zhejiang Ocean University, Zhoushan 316004*

(Received 16 June 2014)

Higher-order localized waves in coupled nonlinear Schrödinger equations are investigated by the generalized Darboux transformation. We show that two dark-bright solitons together with a second-order rogue wave of fundamental or triangular pattern and two breathers together with a second-order rogue wave of fundamental or triangular pattern coexist in the second-order localized wave for the coupled system. Moreover, by increasing the value of one free parameter, the nonlinear waves in the second-order localized wave can merge with each other. The results further reveal the abundant dynamic behaviors of localized waves in coupled systems.

PACS: 02.30.Ik, 05.45.Yv DOI: 10.1088/0256-307X/31/9/090201

Localized waves, including bright or dark solitons, breathers and rogue waves, have become of great interest in the field of nonlinear science in recent decades.[1−6] Compared to the breathers which are localized in space or time (Ma or Akhmediev breathers),[3,4] rogue waves (also known as freak waves) are localized in both space and time, and appear from nowhere and disappear without a trace.[5−9] A wave belongs to this category when its amplitude or steepness reaches several times larger than the average crest, and it is well known that the rational form solution can describe rogue waves in mathematics.[7,10]

Recent studies on localized waves have gradually concentrated on the multi-component coupled systems.[11−19] For instance, in Ref. [14], Baronio *et al.* studied the interactions between a rogue wave and a dark-bright soliton or a breather in the coupled nonlinear Schrödinger (NLS) equations; one free parameter f in their solution plays an important role in controlling the dynamic properties of the localized waves.

In this Letter, motivated by the work of Baronio *et al.*, we consider coupled NLS equations (the Manakov system),

$$iu_t + u_{xx} + 2(|u|^2 + |v|^2)u = 0, \tag{1}$$
$$iv_t + v_{xx} + 2(|u|^2 + |v|^2)v = 0. \tag{2}$$

The coupled NLS equations have been derived as an important model in two-mode or polarized nonlinear optics,[20] and there has been a surge of great interest in studying their integrability and explicit solutions.[10,21−24] Our aim is to generalize Baronio's work[14] into the higher-order case. By using the generalized Darboux transformation (gDT) method,[25−28] a family of higher-order rational and semi-rational solutions are derived for Eqs. (1) and (2). We find that two dark-bright solitons together with a second-order rogue wave of fundamental or triangular pattern and two breathers together with a second-order rogue wave of fundamental or triangular pattern can coexist in the second-order localized wave for the coupled system. Moreover, by increasing the value of α in the solution, the rogue wave and the other nonlinear waves merge with each other.

We start from the Lax pair of Eqs. (1) and (2), which admits

$$\Psi_x = [\zeta U_1 + U_0]\,\Psi, \tag{3}$$
$$\Psi_t = [3\zeta^2 U_1 + 3\zeta U_0 + i\sigma_3(U_{0x} - U_0^2)]\,\Psi, \tag{4}$$

where

$$U_0 = \begin{pmatrix} 0 & u & v \\ -u^* & 0 & 0 \\ -v^* & 0 & 0 \end{pmatrix},$$

$U_1 = \mathrm{diag}\{-2i, i, i\}$, $\sigma_3 = \mathrm{diag}\{1, -1, -1\}$. Here $\Psi = (\psi(x,t), \phi(x,t), \chi(x,t))^T$ is the eigenfunction, and ζ is the spectral parameter. By direct calculation, it is easy to prove that Eqs. (1) and (2) can be exactly reproduced from the compatibility condition of the Lax pair.

In what follows, based on the DT of the Ablowitz–Kaup–Newell–Segur (AKNS) spectral problem,[29,30] the gDT of Eqs. (1) and (2) can be constructed. Let $\Psi_1 = \Psi_1(\zeta_1 + \delta)$ be a basic solution of the Lax pair Eqs. (3) and (4) at $u = u[0]$, $v = v[0]$ and $\zeta = \zeta_1 + \delta$. It is vital that Ψ_1 can be expanded as the Taylor series

*Supported by the National Natural Science Foundation of China under Grant Nos 11275072 and 11326165, the Research Fund for the Doctoral Program of Higher Education of China under Grant No 20120076110024, the Innovative Research Team Program of the National Natural Science Foundation of China under Grant No 61321064, the Shanghai Knowledge Service Platform for Trustworthy Internet of Things under Grant No ZF1213, the Shanghai Minhang District Talents of High Level Scientific Research Project, the Talent Fund and the K.C. Wong Magna Fund in Ningbo University, and the Zhejiang Provincial Natural Science Foundation of China under Grant No LQ12A01008.

**Corresponding author. Email: ychen@sei.ecnu.edu.cn

at $\delta=0$,

$$\begin{aligned}\Psi_1 = &\Psi_1^{[0]} + \Psi_1^{[1]}\delta + \Psi_1^{[2]}\delta^2\\ &+\ldots+\Psi_1^{[N]}\delta^N+\ldots,\end{aligned}\tag{5}$$

where $\Psi_1^{[l]}=(\psi_1^{[l]},\phi_1^{[l]},\chi_1^{[l]})$, $\Psi_1^{[l]}=\frac{1}{l!}\frac{\partial^l\Psi_1}{\partial\delta^l}|_{\delta=0}(l=0,1,2,\ldots)$.

Then the gDT can be defined as the following iterative form

$$\begin{aligned}&\Psi_1[N-1]=\Psi_1^{[0]}+\sum_{l=1}^{N-1}T_1[l]\Psi_1^{[1]}+\sum_{l=1}^{N-1}\sum_{k=1}^{l-1}T_1[l]\\ &\cdot T_1[k]\Psi_1^{[2]}+\ldots+T_1[N-1]T_1[N-2]\\ &\ldots T_1[1]\Psi_1^{[N-1]},\\ &\Psi[N]=T[N]T[N-1]\ldots T[1]\Psi,\\ &T[l]=\zeta I-H[l-1]\Lambda_l H[l-1]^{-1},\end{aligned}\tag{6}$$

$$\begin{aligned}&u[N]=u[N-1]-3i(\zeta_1-\zeta_1^*)\\ &\times\frac{\psi_1[N-1]\phi_1[N-1]^*}{(|\psi_1[N-1]|^2+|\phi_1[N-1]|^2+|\chi_1[N-1]|^2)},\end{aligned}\tag{7}$$

$$\begin{aligned}&v[N]=v[N-1]-3i(\zeta_1-\zeta_1^*)\\ &\times\frac{\psi_1[N-1]\chi_1[N-1]^*}{(|\psi_1[N-1]|^2+|\phi_1[N-1]|^2+|\chi_1[N-1]|^2)},\end{aligned}\tag{8}$$

where $(\psi_1[N-1],\phi_1[N-1],\chi_1[N-1])^T=\Psi_1[N-1]$,

$$H[l-1]=\begin{pmatrix}\psi_1[l-1] & \phi_1[l-1]^* & \chi_1[l-1]^*\\ \phi_1[l-1] & -\psi_1[l-1]^* & 0\\ \chi_1[l-1] & 0 & -\psi_1[l-1]^*\end{pmatrix},$$

and $\Lambda_l=\mathrm{diag}\{\zeta_1,\zeta_1^*,\zeta_1^*\}$, $1\le l\le N$.

It should be remarked that Eqs. (6)–(8) give rise to an Nth-order localized wave solution of Eqs. (1) and (2). In the following, by choosing an adequate eigenfunction Ψ_1, these formulas will be applied to generate localized wave solutions of Eqs. (1) and (2).

In the following, we begin with a nontrivial seed solution to Eqs. (1) and (2),

$$u[0]=d_1e^{2i\theta},\ v[0]=d_2e^{2i\theta},\tag{9}$$

where d_1 and d_2 are real constants, $\theta=(d_1^2+d_2^2)t$. Then the solution of the Lax pair Eqs. (3) and (4) at $u=u[0]$ and $v=v[0]$ can be chosen as

$$\Psi_1=\begin{pmatrix}(C_1e^{M_1+M_2}-C_2e^{M_1-M_2})e^{i\theta}\\ \rho_1(C_1e^{M_1-M_2}-C_2e^{M_1+M_2})e^{-i\theta}+d_2\alpha e^{M_3}\\ \rho_2(C_1e^{M_1-M_2}-C_2e^{M_1+M_2})e^{-i\theta}-d_1\alpha e^{M_3}\end{pmatrix},\tag{10}$$

where

$$\begin{aligned}&C_1=\frac{[3\zeta-\sqrt{9\zeta^2+4(d_1^2+d_2^2)}]^{\frac12}}{\sqrt{9\zeta^2+4(d_1^2+d_2^2)}},\\ &C_2=\frac{[3\zeta+\sqrt{9\zeta^2+4(d_1^2+d_2^2)}]^{\frac12}}{\sqrt{9\zeta^2+4(d_1^2+d_2^2)}},\\ &\rho_1=\frac{d_1}{\sqrt{d_1^2+d_2^2}},\\ &\rho_2=\frac{d_2}{\sqrt{d_1^2+d_2^2}},\\ &M_1=-\frac12 i\zeta(x+3\zeta t),\ M_3=i\zeta(x+3\zeta t),\\ &M_2=\frac12 i\sqrt{9\zeta^2+4(d_1^2+d_2^2)}(x+3\zeta t+\sum_{k=1}^N s_kf^{2k}),\end{aligned}$$

where $s_k=m_k+in_k,(1\le k\le N)$, α, m_k, n_k are real free parameters, and f is a small parameter.

Letting $\tau=d_1^2+d_2^2$ and $\zeta=\frac23 i\sqrt{\tau}(1+f^2)$, then expanding the vector function $\Psi_1(f)$ at $f=0$, we can calculate

$$\Psi_1(f)=\Psi_1^{[0]}+\Psi_1^{[1]}f^2+\ldots,\tag{11}$$

where

$$\begin{aligned}\psi_1^{[0]}=&\frac{(i-1)}{2\tau^{1/4}}[2\sqrt{\tau}x+4i\tau t+1]e^{\xi_1},\\ \phi_1^{[0]}=&-\frac{(i-1)d_1}{2\tau^{3/4}}[2\sqrt{\tau}x+4i\tau t-1]e^{\xi_2}+d_2\alpha e^{\xi_3},\\ \chi_1^{[0]}=&-\frac{(i-1)d_2}{2\tau^{3/4}}[2\sqrt{\tau}x+4i\tau t-1]e^{\xi_2}-d_1\alpha e^{\xi_3},\\ \psi_1^{[1]}=&\frac{(i-1)}{24\tau^{1/4}}[8\tau^{3/2}x^3+20\tau x^2+10\sqrt{\tau}x-(96\tau^{5/2}x\\ &+112\tau^2)t^2+24\sqrt{\tau}m_1+24\sqrt{\tau}n_1-3+i(-64\tau^3t^3\\ &+(48\tau^2x^2+96\tau^{3/2}x+76\tau)t)]e^{\xi_1},\\ \phi_1^{[1]}=&\frac{(i-1)d_1}{24\tau^{3/4}}[-8\tau^{3/2}x^3+4\tau x^2-2\sqrt{\tau}x+(96\tau^{5/2}x\\ &+16\tau^2)t^2-24\sqrt{\tau}m_1-24\sqrt{\tau}n_1-3\\ &+i(64\tau^3t^3-(48\tau^2x^2+44\tau)t)]e^{\xi_2}\\ &-\frac23 d_2\alpha(\sqrt{\tau}x+4i\tau t)e^{\xi_3},\\ \chi_1^{[1]}=&\frac{(i-1)d_2}{24\tau^{3/4}}[-8\tau^{3/2}x^3+4\tau x^2-2\sqrt{\tau}x+(96\tau^{5/2}x\\ &+16\tau^2)t^2-24\sqrt{\tau}m_1-24\sqrt{\tau}n_1-3+i(64\tau^3t^3\\ &-(48\tau^2x^2+44\tau)t)]e^{\xi_2}+\frac23 d_1\alpha(\sqrt{\tau}x+4i\tau t)e^{\xi_3},\\ &\ldots\end{aligned}$$

with

$$\begin{aligned}\xi_1=&\frac13\sqrt{\tau}x+\frac53 i\tau t,\\ \xi_2=&\frac13\sqrt{\tau}x-\frac13 i\tau t,\\ \xi_3=&-\frac23\sqrt{\tau}(x+2i\sqrt{\tau}t).\end{aligned}$$

It is straightforward to verify that $\Psi_1^{[0]}$ is a solution of the Lax pair Eqs. (3) and (4) at $u = u[0]$, $v = v[0]$ and $\zeta = \zeta_1 = \frac{2}{3}i\sqrt{\tau}$. Hence, from the first-step gDT, we arrive at

$$u[1] = d_1e^{2i\theta} + \frac{d_1(F_1 + iG_1)e^{2i\theta} + d_2\alpha\tau^{3/4}H_1e^{\eta_1}}{D_1 + \tau^{3/2}\alpha^2e^{\eta_2}}, \tag{12}$$

$$v[1] = d_2e^{2i\theta} + \frac{d_2(F_1 + iG_1)e^{2i\theta} - d_1\alpha\tau^{3/4}H_1e^{\eta_1}}{D_1 + \tau^{3/2}\alpha^2e^{\eta_2}}, \tag{13}$$

where

$$\begin{aligned} F_1 &= -8\tau x^2 - 32\tau^2t^2 + 2,\ G_1 = 16\tau t,\\ H_1 &= 2(i-1)(2\sqrt{\tau}x + 4i\tau t + 1),\\ \eta_1 &= -\sqrt{\tau}x + 3i\tau t,\\ D_1 &= 4\tau x^2 + 16\tau^2t^2 + 1,\ \eta_2 = -2\sqrt{\tau}x. \end{aligned}$$

The validity of the above solution can be directly verified by putting it back into Eqs. (1) and (2). At this point, we obtain the first-order localized wave solution with a semi-rational, multi-parameter form that has been studied by Baronio *et al.*[14] The parameter α plays an important role in controlling the dynamics of the localized wave.

After that, by substituting the explicit expressions of $\Psi_1^{[0]}$ and $\Psi_1^{[1]}$ in Eq. (11) into the following limit

$$\begin{aligned} &\lim_{f\to 0}\frac{T[1]|_{\zeta=\frac{2}{3}i\sqrt{\tau}(1+f^2)}\Psi_1}{f^2}\\ &=\lim_{f\to 0}\frac{(\frac{2}{3}i\sqrt{\tau}f^2 + T_1[1])\Psi_1}{f^2}\\ &=\frac{2}{3}i\sqrt{\tau}\Psi_1^{[0]} + T_1[1]\Psi_1^{[1]} \equiv \Psi_1[1], \end{aligned} \tag{14}$$

together with Eq. (6) with $N = 1$, and Eqs. (7) and (8) with $N = 2$, the more complicated second-order localized wave solution can be derived. Here we omit the concrete expressions of $u[2]$ and $v[2]$, since it is quite cumbersome to write them down here, although it is not difficult to verify their validity with the help of Maple. Next, we discuss the dynamics of the higher-order localized waves.

(i) When $\alpha = 0$, $u[2]$ is proportional to $v[2]$, which can be seen as the vector generalization of the second-order rogue wave solution of the scalar NLS equation, and has been studied by Zhai *et al.*[23]

(ii) When $\alpha \neq 0$, $d_1 \neq 0$ and $d_2 = 0$, the second-order dark-bright-rogue wave solution can be obtained. We see that in Figs. 1 and 2, two dark-bright solitons together with a second-order rogue wave of fundamental pattern and triangular pattern coexist in the second-order localized wave, respectively. In Fig. 1(a), the maximum amplitude of the localized wave in the u component is five and occurs at $(0, 0)$. In Fig. 2(a), there are three highest humps in the localized wave, their amplitudes are 2.9225, 3.0304, 3.0304, and arrive at $(3.5569, 0)$, $(-1.8776, 1.4540)$, $(-1.8776, -1.4540)$, respectively. While considering the zero-amplitude background crest, the rogue wave in the v component is difficult to observe because of its small amplitude, see Figs. 1(b) and 2(b). Furthermore, by increasing the value of α, the rogue wave and the dark-bright solitons merge with each other, see Fig. 3. The maximum amplitude of the localized wave in the u component is 2.6728 and occurs at $(0.0743, 0)$, in the v component it is 3.6588 and occurs at $(0.1594, 0)$.

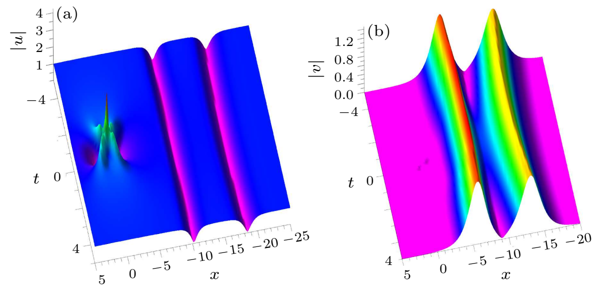

Fig. 1. Evolution plot of the second-order dark-bright-rogue waves in coupled NLS equations by choosing $d_1 = 1$, $d_2 = 0$ and $s_1 = 0$. (a) The u component with $\alpha = 1/10000$; (b) the v component with $\alpha = 1/100$.

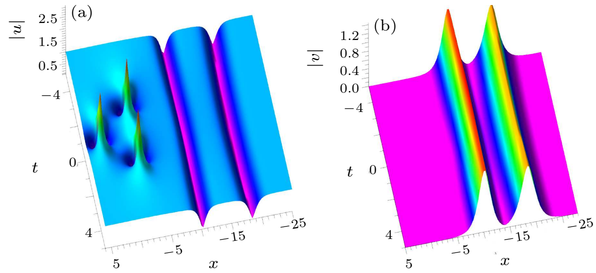

Fig. 2. Evolution plot of the second-order dark-bright-rogue waves in coupled NLS equations by choosing $d_1 = 1$, $d_2 = 0$, $s_1 = 30$ and $\alpha = 1/10000$. (a) The u component and (b) the v component.

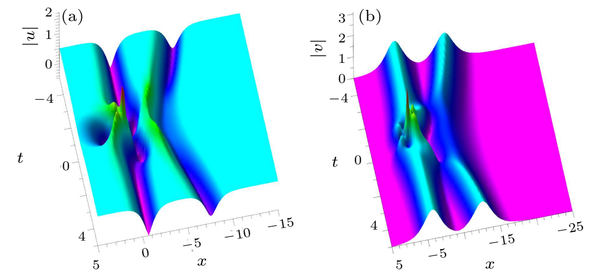

Fig. 3. Evolution plot of the second-order dark-bright-rogue waves in coupled NLS equations by choosing $d_1 = 1$, $d_2 = 0$, $s_1 = 0$ and $\alpha = 1$. (a) The u component and (b) the v component.

(iii) When $\alpha \neq 0$, $d_1 \neq 0$, $d_2 \neq 0$, the second-order breather-rogue wave solution can be obtained. In Figs. 4 and 5, we notice that two breathers together with a second-order rogue wave of fundamental pattern and triangular pattern coexist in the second-order localized waves, respectively. In Fig. 4, the maximum amplitudes of the localized waves in the u component and v component both are five and arrive at $(0,0)$. In Fig. 5(a), there are three highest humps in the localized wave, their amplitudes are 2.9558, 3.0130, 3.0008, and occur at $(3.3472, 0)$, $(-1.7279, -0.9916)$, $(-1.7281, 0.9917)$, respectively. In Fig. 5(b), the three humps appear at $(3.3472, 0)$, $(-1.7273, 0.9916)$, $(-1.7275, -0.9917)$, and their amplitudes are 2.9559, 3.0401, 3.0280, respectively. By increasing the value of α, we observe that in Fig. 6, the rogue wave and the breathers merge with each other. The maximum amplitude of the localized wave in the u component is 2.6303 and arrives at $(-0.3510, -0.1271)$, in the v component it is 5.1516 and arrives at $(0.1472, -0.0005)$.

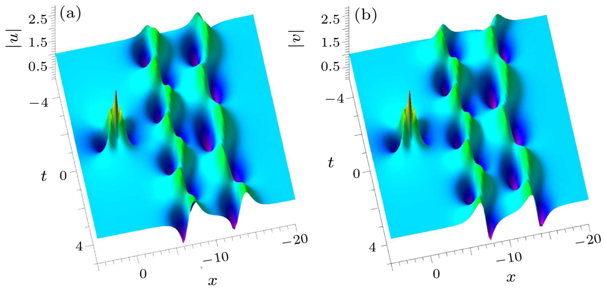

Fig. 4. Evolution plot of the second-order breather-rogue waves in coupled NLS equations by choosing $d_1 = 1$, $d_2 = 1$, $\alpha = 1/10000$ and $s_1 = 0$. (a) The u component and (b) the v component.

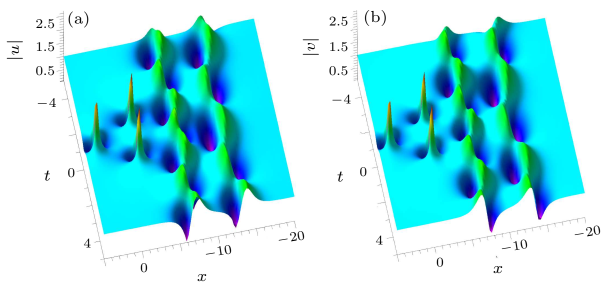

Fig. 5. Evolution plot of the second-order breather-rogue waves in coupled NLS equations by choosing $d_1 = 1$, $d_2 = 1$, $\alpha = 1/10000$ and $s_1 = 50$. (a) The u component and (b) the v component.

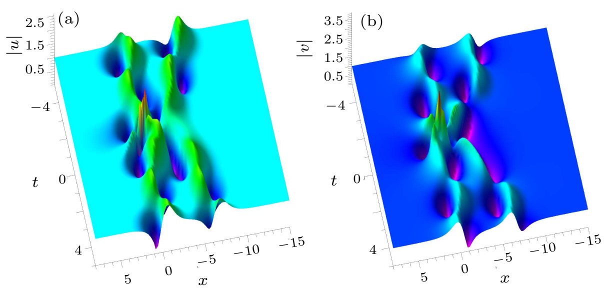

Fig. 6. Evolution plot of the second-order breather-rogue waves in coupled NLS equations by choosing $d_1 = 1$, $d_2 = 1$, $\alpha = 1$ and $s_1 = 0$. (a) The u component and (b) the v component.

In conclusion, we generalize Baronio's work into the higher-order case by the gDT method. Some interesting higher-order localized waves are explicitly shown in Figs. 1–6. Our results further reveal the striking dynamic structures of localized waves in a coupled system, and we hope the higher-order localized waves presented in this work will be verified in physical experiments in the future.

References

[1] Khaykovich L, Schreck F et al 2002 *Science* **296** 1290
[2] Burger S, Bongs K et al 1999 *Phys. Rev. Lett.* **83** 5198
[3] Ma Y C 1979 *Stud. Appl. Math.* **60** 43
[4] Akhmediev N, Eleonskii V M and Kulagin N E 1987 *Theor. Math. Phys.* **72** 183
[5] Peregrine D H and Austral J 1983 *J. Aust. Math. Soc. Ser.* B **25** 16
[6] Akhmediev N, Ankiewicz A and Taki M 2009 *Phys. Lett.* A **373** 675
[7] Akhmediev N, Ankiewicz A and Soto-Crespo J M 2009 *Phys. Rev.* E **80** 026601
[8] Kedziora D J, Ankiewicz A and Akhmediev N 2011 *Phys. Rev.* E **84** 056611
[9] He J S, Zhang H R, Wang L H, Porsezian K and Fokas A S 2013 *Phys. Rev.* E **87** 052914
[10] Priya N V, Senthilvelan M and Lakshmanan M 2013 *Phys. Rev.* E **88** 022918
[11] Bludov Y V, Konotop V V and Akhmediev N 2010 *Eur. Phys. J. Spec. Top.* **185** 169
[12] Zhao L C and Liu J 2013 *Phys. Rev.* E **87** 013201
[13] Baronio F, Conforti M, Degasperis A and Lombardo S 2013 *Phys. Rev. Lett.* **111** 114101
[14] Baronio F, Degasperis A, Conforti M and Wabnitz S 2012 *Phys. Rev. Lett.* **109** 044102
[15] Guo B L and Ling L M 2011 *Chin. Phys. Lett.* **28** 110202
[16] Zhao L C and Liu J 2012 *J. Opt. Soc. Am.* B **29** 3119
[17] Degasperis A and Lombardo S 2013 *Phys. Rev.* E **88** 052914
[18] Wang X and Chen Y 2014 *Chin. Phys.* B **23** 070203
[19] Mu G, Qin Z Y and Grimshaw R 2014 arXiv:1404.2988
[20] Tang D Y, Zhang H, Zhao L M and Wu X 2008 *Phys. Rev. Lett.* **101** 153904
[21] Manakov S V 1973 *Zh. Eksp. Teor. Fiz.* **65** 505
[22] Ling L M, Guo B L and Zhao L C 2014 *Phys. Rev.* E **89** 041201
[23] Zhai B G, Zhang W G, Wang X L and Zhang H Q 2013 *Nonlinear Anal.: Real World Appl.* **14** 14
[24] Qiao Z J and Zhao X Y 1991 *Acta Inner Mongolia Nationality University* **9** 16
[25] Guo B L, Ling L M and Liu Q P 2012 *Phys. Rev.* E **85** 026607
[26] Guo B L, Ling L M and Liu Q P 2013 *Stud. Appl. Math.* **130** 317
[27] Yang B, Zhang W G, Zhang H Q and Pei S B 2013 *Phys. Scr.* **88** 065004
[28] Wang X, Li Y Q and Chen Y 2013 *Commun. Nonlinear Sci. Numer. Simul.* (accepted) arXiv:1312.6479
[29] Gu C H, Hu H S and Zhou Z X 2005 *Darboux Transformations in Integrable Systems: Theory and Their Applications to Geometry* (New York: Springer-Verlag)
[30] Matveev V B and Salle M A 1991 *Darboux Transformations and Solitons* (Berlin: Springer-Verlag)